Partial Slip Effects on MHD Peristaltic Flow of Carreau-Yasuda Fluid (CY) Through a Planner Micro-Channel

Hanumesh Vaidya[1], Kerehalli Vinayaka Prasad[1], Rajashekhar Choudhari[2,*], Shivaleela[1], Shivaraya Keriyappa[1], Manjunatha Gudekote[3], Jyoti Shetty[2]

[1] Department of Mathematics, Vijayanagara Sri Krishnadevaraya University, Ballari, Karnataka, India
[2] Department of Mathematics, Manipal Institute of Technology Bengaluru, Manipal Academy of Higher Education, Manipal, Karnataka, India
[3] Department of Mathematics, Manipal Institute of Technology, Manipal Academy of Higher Education, Manipal, Karnataka, India

ARTICLE INFO	ABSTRACT
	In modern applied mathematics, engineering, and the physiological world, the concept of peristalsis is of great significance. The present article concentrates on the peristaltic movement of Carreau-Yasuda fluid through planner micro-channel under the influence of applied magnetic field and partial slip conditions. The governing system of equations are nondimensionalized and transformed using basic assumptions such as long wavelength and low Reynolds number. A bulti-in route "ND solve" in Mathematica exercised to solve obtained nonlinear coupled equations with appropriate boundary conditions. Obtained results are elucidated by plotting graphs for different physiological constraints such as velocity, temperature, and concentration. Physical characteristics such as skin friction, Nusselt number and Sherwood number are discussed via table results. The typical character of this work e.g. flow index parameter exhibits that the apparent fluid viscosity becomes high when it has a higher value due to which fluid faces more resistance and the presence of a higher magnetic effect predicts the decreasing behavior on velocity. Additionally, the trapping phenomenon explains bolus movement and are discussed briefly.

1. Introduction

In the last few decades, many investigations have shown more interest in the transportation of biological fluids through different mathematical geometries because the fluid flow is generated in wavy form *i.e.* wavy mechanism (peristaltic mechanism), which has enormous applications in biomechanics and engineering areas, etc. Such kinds of transportation occur during urine transport through the ureter, food movement through the esophagus, blood circulation, toxic liquid transportation in nuclear industries, vasomotion of small blood vessels such as capillary arteries and veins, worm motility, deadly cell treatment and bleeding reduction throughout the operation, etc.

Corresponding author.
E-mail address: rv.choudhari@manipal.edu

This process is also used to produce dialysis devices, ventilators, open-heart bypass pumps, fusion pumps, etc. and in the study and treatment of diagnostic issues in living organisms.

Owing to all the above insights, the core concept of peristaltic flow was introduced by Latham [1]. Primarily, he worked on viscous fluids (urine flow through the ureter). Early investigations were carried out on peristalsis using Newtonian fluids with different geometries Burns and Parkes [2]. Assumptions of low Reynold's number and long wavelength approximations were studied by Shapiro *et al.,* [3], which was used to examine the mean flow rate under distinct boundary conditions and reflux flow in biological organs like the ureter and gastrointestinal tract etc. However, the premise of a Newtonian approach in modeling the peristaltic mechanism might not be adequate to understand the complex rheological activity of non-Newtonian fluids. By considering non-Newtonian fluids, Raju and Devanathan [4] started work on the power-law fluid model that discussed the flow of the blood in peristalsis. Continuing, Girija Devi and Devanathan [5] worked on micropolar fluid. Srivastava and Srivastava [6] investigate the blood flow through uniform and non-uniform tubes in the Casson fluid model. Vajravelu *et al.,* [7] utilized the approximations in the peristaltic mechanism. Later, plenty of investigations were established on the peristalsis mechanism with various fluid models that explore the flow complexity of Newtonian and non-Newtonian fluids in different suppositions [8-11].

The analysis of the non-Newtonian fluid model gained huge prominence in discrete areas like industries and medical fields etc. Because the presence of viscoelastic properties in fluids helps to understand the complexity behind the fluid flow, among those models, the Carreau-Yasuda fluid model predicts extensive application in the research area. This model's main utility is to predict blood's shear thickening and shear thinning behaviours. In its limiting case, it can predict Newtonian and Carreau fluid models. Also, it explains five parameters to understand the rheological behaviour of fluid when compared with the three constants of the power law model. Furthermore, this model is also used in the manufacturing industry, like pumping equipment, which works better than Newtonian fluids and medical equipment design. Many examinations were carried out on the CY fluid model due to all the above visions. Non-Newtonian properties of blood flow in arteries were analyzed by Gijsen *et al.,* [12] using both numerical data and experimental data results.

Further, Abbasi *et al.,* [13] investigate the significance of CY fluid flow through the asymmetric channel. In continuing, Hayat *et al.,* [14] reported the numerical investigation of MHD Carreau-Yasuda fluid. Kayani *et al.,* [15] examined the influence of wall properties on CY model. A calendaring process using Carreau-Yasuda fluid was discussed numerically by Javed *et al.,* [16]. The induced effect of the Carreau Fluid Model on different cells and Pressure Gradient at the Ampullar Region Entrance was reported by Arshaf *et al.,* [17]. Later on, numerous surveys started to elaborate the concepts of the Carreau Yasuda fluid model in different suppositions [18-41].

Inspired by the views mentioned earlier, the present work intended to explore Ref. [42], which explained the impact of the Carreau fluid model in the absence of a magnetitic effect. The current work explores the model by considering the Carreau-Yasuda (CY) fluid model, which can predict the Carreau fluid and Newtonian models. Primarily, the pumping equipment works better compared to Newtonian fluids. Additionally, the partial slip effects are discussed on MHD peristaltic flow. Such a dimension of investigation has not yet been discussed. The present work has credible appliances in medicine and biomedical engineering. Especially in biomedical industries, it has a significant role in advancing and improving different kinds of drug delivery machines.

2. Mathematical Formulation

2.1 Flow Regime

Consider a two-dimensional peristaltic flow of an incompressible Carreau-Yasuda fluid (CY) in a microchannel of width $2\bar{a}$ and $\bar{Y} = \pm\bar{h}\left(\bar{X}, \bar{t}\right)$ considered as lower and upper wall respectively. The unsteady and laminar flow of the fluid is generated on the walls of the channel when sinusoidal waves are created along with the walls having large wavelength (compared with the mean channel width) and wave speed c. The fluid flow is maintained by providing temperature and concentration as T_0, C_0, T_1 and C_1 to both the upper and lower walls respectively. The geometry of the microchannel wall can be expressed mathematically as

$$\bar{Y} = \pm\bar{h}\left(\bar{X}, \bar{t}\right) = \pm\left(\bar{a} + \bar{b}\,Sin\left(\frac{2\pi\left(\bar{X} - c\bar{t}\right)}{\lambda}\right)\right) \tag{1}$$

where, $\left(\bar{X}, \bar{Y}\right)$ are axial and transverse coordinates. $\bar{a}, \bar{b}, c, \lambda$ and $\bar{t}$ are represent the half-width of the channel, amplitude of the channel, speed of the wave, wavelength and time respectively.
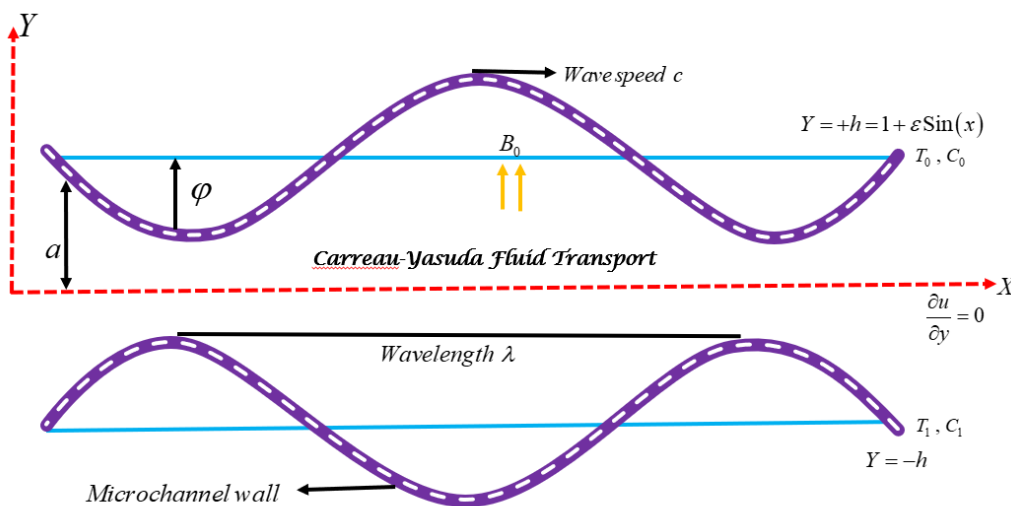
Fig. 1. Geometry of the fluid flow

The expressions for non-Newtonian Carreau-Yasuda fluid are given by

$$\bar{S} = \mu(\dot{\gamma})\bar{A}_1 \tag{2}$$

where, $\mu(\dot{\gamma})$ is the apparent viscosity. The Lorenz force by using ohm's law is given by

$$J \times B = \left(0, -\sigma B_0^2\left(\bar{V} + m\bar{U}\right), 0\right) \tag{3}$$

where J is the current density and B is the magnetic field.

2.2 Governing Equations

The governing equations in the laboratory frame for a Carreau-Yasuda fluid as follows

$$\frac{\partial \overline{U}}{\partial \overline{X}} + \frac{\partial \overline{V}}{\partial \overline{Y}} = 0 \tag{4}$$

$$\rho \left(\frac{\partial \overline{U}}{\partial \overline{t}} + \overline{U} \frac{\partial \overline{U}}{\partial \overline{X}} + \overline{V} \frac{\partial \overline{U}}{\partial \overline{Y}} \right) = -\frac{\partial \overline{p}}{\partial \overline{X}} + \frac{\partial}{\partial \overline{Y}} \overline{\tau}_{\overline{X}\overline{Y}} + \frac{\partial}{\partial \overline{X}} \overline{\tau}_{\overline{X}\overline{X}} - \sigma B_0^2 \left(\overline{U} + c \right) \tag{5}$$

$$\rho \left(\frac{\partial \overline{V}}{\partial \overline{t}} + \overline{U} \frac{\partial \overline{V}}{\partial \overline{X}} + \overline{V} \frac{\partial \overline{V}}{\partial \overline{Y}} \right) = -\frac{\partial \overline{p}}{\partial \overline{Y}} + \frac{\partial}{\partial \overline{X}} \overline{\tau}_{\overline{X}\overline{Y}} + \frac{\partial}{\partial \overline{Y}} \overline{\tau}_{\overline{Y}\overline{Y}} \tag{6}$$

$$\rho c_p \left(\frac{d\overline{T}}{d\overline{t}} + \overline{U} \frac{d\overline{T}}{d\overline{X}} + \overline{V} \frac{d\overline{T}}{d\overline{Y}} \right) = k \left(\frac{\partial^2 \overline{T}}{\partial \overline{X}^2} + \frac{\partial^2 \overline{T}}{\partial \overline{Y}^2} \right) + \left(\frac{\partial \overline{U}}{\partial \overline{X}} \overline{\tau}_{\overline{X}\overline{X}} + \frac{\partial \overline{V}}{\partial \overline{Y}} \overline{\tau}_{\overline{Y}\overline{Y}} + \left(\frac{\partial \overline{U}}{\partial \overline{Y}} + \frac{\partial \overline{V}}{\partial \overline{X}} \right) \overline{\tau}_{\overline{X}\overline{Y}} \right) \tag{7}$$

$$\left(\frac{\partial \overline{C}}{\partial \overline{t}} + \overline{U} \frac{\partial \overline{C}}{\partial \overline{X}} + \overline{V} \frac{\partial \overline{C}}{\partial \overline{Y}} \right) = D_m \left(\frac{\partial^2 \overline{C}}{\partial \overline{X}^2} + \frac{\partial^2 \overline{C}}{\partial \overline{Y}^2} \right) + \frac{k_t D_m}{T_m} \left(\frac{\partial^2 \overline{T}}{\partial \overline{X}^2} + \frac{\partial^2 \overline{T}}{\partial \overline{Y}^2} \right) \tag{8}$$

Here, $\left(\overline{U}, \overline{V} \right)$ are the velocity coordinates along with $\left(\overline{X}, \overline{Y} \right)$ direction respectively. $\overline{p}$, ρ, c_p, k, k_t, D_m, T_m, $\overline{T}$ and $\overline{C}$ represents pressure, fluid density, specific heat, thermal conductivity, ratio of thermal diffusion, mass diffusivity co-efficient, mean temperature, temperature, and concentration of the field respectively.

2.3 Nondimensionalisation

The equations in the form of fixed coordinate system $\left(\overline{X}, \overline{Y} \right)$ are transformed to moving coordinate system $(\overline{x}, \overline{y})$ is as follows

$$\overline{x} = \overline{X} - c\overline{t}, \, \overline{y} = \overline{Y}, \overline{u} \left(\overline{x}, \overline{y} \right) = \overline{U} \left(\overline{X}, \overline{Y}, \overline{t} \right) - c, \overline{v} \left(\overline{x}, \overline{y} \right) = \overline{V} \left(\overline{X}, \overline{Y}, \overline{t} \right),$$
$$\overline{p} \left(\overline{x}, \overline{y} \right) = \overline{P}(\overline{X}, \overline{Y}, \overline{t}), T \left(\overline{x}, \overline{y} \right) = \overline{T} \left(\overline{X}, \overline{Y}, \overline{t} \right) \tag{9}$$

Employing these transformations and introducing the following non-dimensional variables

$$x = \frac{2\pi \bar{x}}{\lambda}, y = \frac{\bar{y}}{a}, u = \frac{\bar{u}}{c}, t = \frac{2\pi c \bar{t}}{\lambda}, p = \frac{2\pi \bar{p} a^2}{\lambda \mu c}, a = \frac{2\pi \bar{a}}{\lambda}, b = \frac{b_1}{d_1}, h = \frac{\bar{h}}{a}, \Pr = \frac{\mu c_p}{k},$$

$$\varepsilon = \frac{b}{a}, \theta = \frac{\bar{T} - \bar{T}_0}{\bar{T}_0}, \Omega = \frac{\bar{C} - \bar{C}_0}{\bar{C}_0}, \mathrm{Mn} = \sqrt{\frac{\sigma}{\mu}} B_0 a, \psi = \frac{\bar{\psi}}{ca}, u = \frac{\partial \psi}{\partial y}, v = -\alpha \frac{\partial \psi}{\partial y}, \quad (10)$$

$$Br = Ec\Pr, \mathrm{Re} = \frac{\rho c a}{\mu}, f = \frac{\bar{q}}{ca}, \Theta = \frac{\bar{Q}}{ca}, Sr = \frac{T_0 k_t D_m}{v T_m C_0}, Sc = \frac{v}{D_m}, \tau_{XY} = \frac{\bar{\tau}_{\bar{X}\bar{Y}} a_1}{\mu c}, Ec = \frac{c^2}{c_p T_0}.$$

Here, (x, y) are non-dimensional axial and transverse coordinates. p, α, Θ, θ, Ω, ψ, Br, Re, Pr, ε, Sr, Sc, Mn and Ec are the non-dimensional parameters such as pressure, peristaltic wave number, dimensionless volume flow rate, dimensionless temperature, dimensionless concentration, non-dimensional shear stress, Brinkmann number, Reynolds number, Prandtl number, amplitude ratio, non-dimensional Soret number, Schmidt number, Magnetic parameter and Eckert number respectively. The dimensionless shear stress τ_{XY} is obtained as follows

$$\tau_{XY} = \left(\left(1 + \frac{n-1}{a} We^a \left(\frac{\partial^2 \psi}{\partial y^2} \right)^a \right) \frac{\partial^2 \psi}{\partial y^2} \right) \quad (11)$$

By using approximations of long-wavelength and low Reynolds number and ignoring higher order of α, we get a transformed system of equations which are substituted by Eq. (11) and are expressed as

$$\frac{dp}{dx} = \frac{\partial}{\partial y} \left(\left(1 + \frac{n-1}{a} We^a \left(\frac{\partial^2 \psi}{\partial y^2} \right)^a \right) \frac{\partial^2 \psi}{\partial y^2} - Mn^2 \left(\frac{\partial \psi}{\partial y} + 1 \right) \right) \quad (12)$$

$$\frac{\partial p}{\partial y} = 0 \quad (13)$$

$$\frac{\partial}{\partial y} \left(\frac{\partial \theta}{\partial y} \right) + Br \left(1 + \frac{n-1}{a} We^a \left(\frac{\partial^2 \psi}{\partial y^2} \right)^a \right) \left(\frac{\partial^2 \psi}{\partial y^2} \right)^2 = 0 \quad (14)$$

$$\frac{d^2 \Omega}{dy^2} + Sc\, Sr \frac{d^2 \theta}{dy^2} = 0 \quad (15)$$

Eliminating pressure from Eq. (12), we obtain the following

$$\frac{\partial^2}{\partial y^2} \left(\left(1 + \frac{n-1}{a} We^a \left(\frac{\partial^2 \psi}{\partial y^2} \right)^a \right) \frac{\partial^2 \psi}{\partial y^2} \right) - Mn^2 \frac{\partial^2 \psi}{\partial y^2} = 0 \quad (16)$$

Correspondingly, the constructed boundary assumptions are

$$\psi = 0, \frac{d^2\psi}{dy^2} = 0, \theta = 0, \Omega = 0, \text{ at } y = 0$$

$$\psi = f, \frac{d\psi}{dy} + \alpha \frac{d^2\psi}{dy^2} = -1, B_h \theta + \frac{d\theta}{dy} = 1, B_m \Omega + \frac{d\Omega}{dy} = 1 \text{ at } y = h = 1 + \varepsilon Sin(x)$$

(17)

Here, B_h and B_m are convective heat and mass transfer parameters respectively. The relation between Θ (dimensionless flow rate in the fixed frame) and f (dimensionless flow rate in the moving frame) is expressed as

$$\Theta = f + 1.$$

(18)

The wall shear stress (skin-friction co-efficient), heat transfer co-efficient (Nusselt number), and mass transfer co-efficient (Sherwood number) in non-dimensional form is given by

$$C_f = h' \frac{\partial^2\psi}{\partial y^2}\bigg|_{y=h}, Nu = h' \frac{\partial\theta}{\partial y}\bigg|_{y=h}, Sh = h' \frac{\partial\Omega}{\partial y}\bigg|_{y=h}$$

(19)

The nonlinear system of equations Eq. (12) to Eq. (16) with appropriate boundary conditions Eq. (17) are solved for different physiological constraints such as velocity, temperature distribution, concentration, skin-friction coefficient, Nusselt number, Sherwood number and stream function by means of built-in routine ND Solve in Mathematica.

3. Results and Discussion

The main purpose of this section is to discuss the impact of various physical constraints on velocity, temperature and concentration. Also, the flow pattern of the bolus is discussed through streamline graphs for different pertinent parameters.

3.1 Flow Characteristics

This subsection aims to deliberate the effect of appropriate physical parameters on the velocity profile shown in Figure 2(a)-(d). Figure 2(a) depicts the impact of Mn on velocity, which shows a declining effect by the higher value of the Mn due to the presence of Lorenz force which resists the fluid flow. Similarly, the impact of n also shows the same effect as that of Mn. This highlights the fact that the apparent fluid viscosity becomes high, due to which fluid faces more opposition. Therefore, the velocity profile increases by hiking the values of n Figure 2(b). To understand the impact of the Weissenberg parameter on velocity Figure 2(c) is obtained, which depicts increasing effect by enlarging values of We. Figure 2(d) predicts variation of the velocity slip parameter that shows a decaying of the velocity profile by enhancing values of the velocity slip parameter.
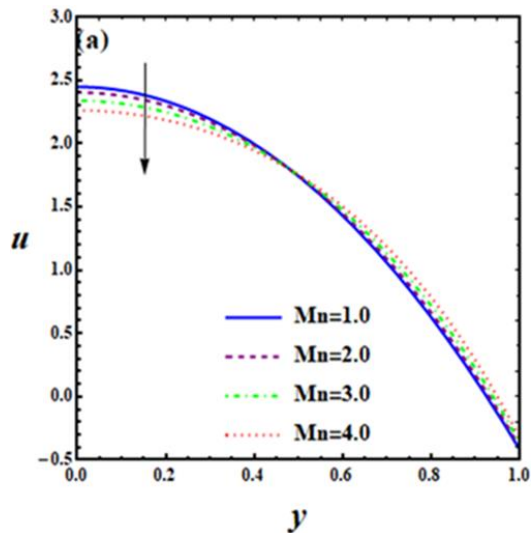
Fig. 2(a). Velocity profile for different values of Mn
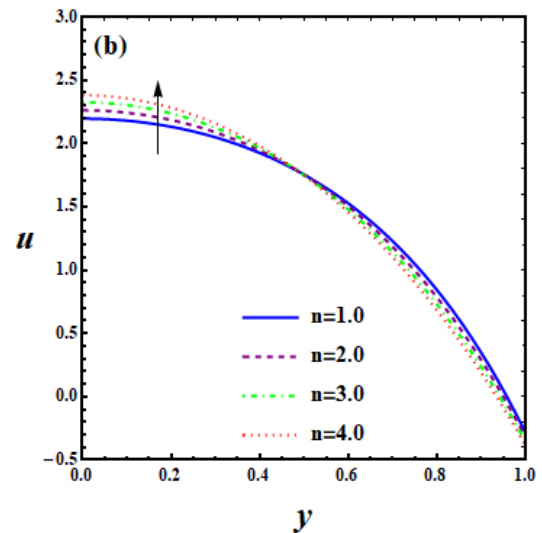
Fig. 2(b). Velocity profile for different values of n
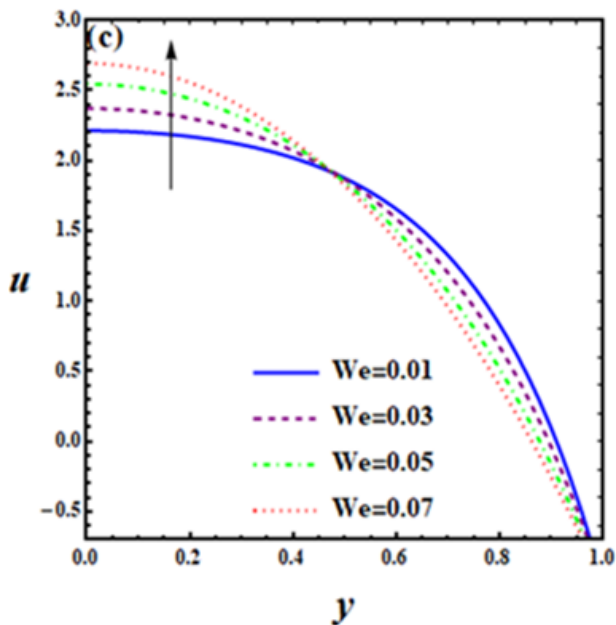
Fig. 2(c). Velocity profile for different values of We
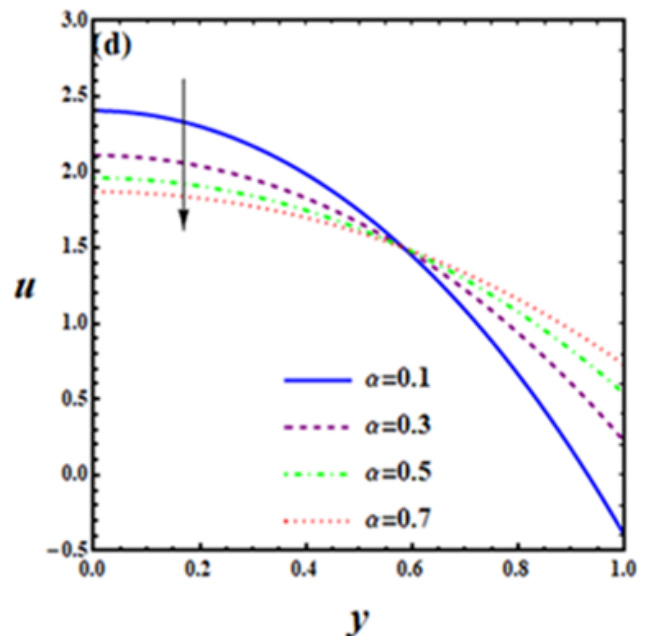
Fig. 2(d). Velocity profile for different values of α

3.2 Heat Characteristics

Temperature distribution of various physical constraints are plotted in Figure 3(a)-(e). The variation of the magnetic parameter is explained in Figure 3(a) that shows decreasing effect by hiking values of Mn parameter. The Figure 3(b) explains the impact of n (flow behavior index) parameter on the temperature profile, which shows a similar behavior as Mn. From Figure 3(c), by increasing values of Weissenberg parameter (We), shows decreasing effect on the temperature profile. But Brickman parameter shows the contrary effect of We i.e., Figure 3(d). The Figure 3(e) explains the impact of convective heat parameter B_h on temperature profile which explain the variation of heat.
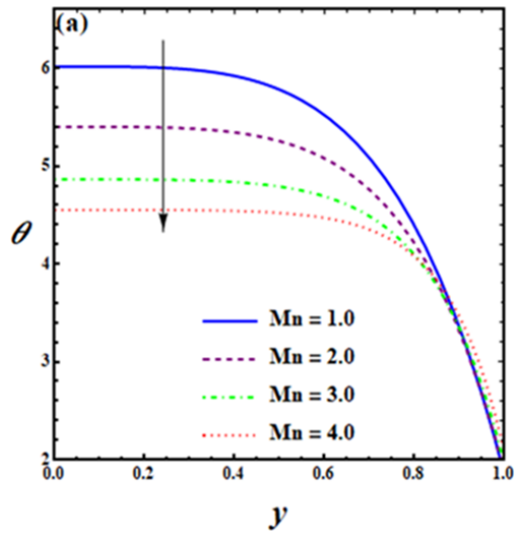
Fig. 3(a). Temperature profile for different values of Mn
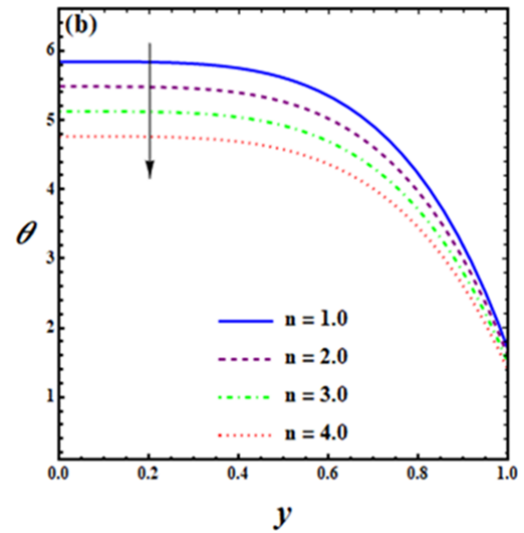
Fig. 3(b). Temperature profile for different values of n
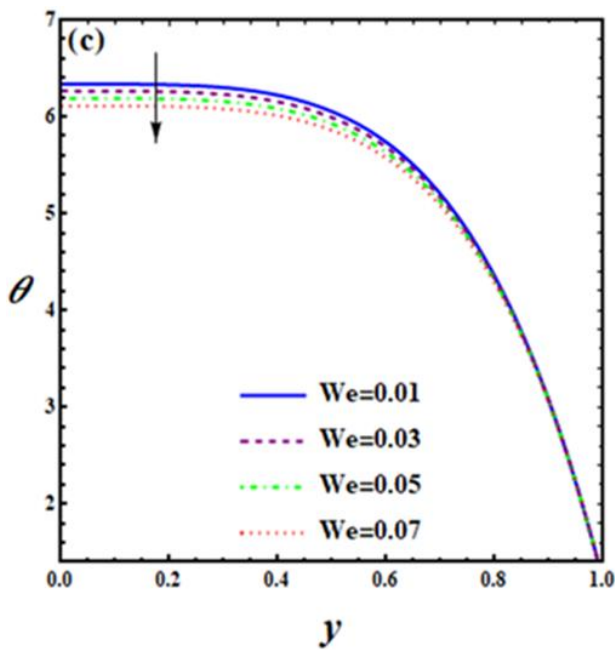
Fig. 3(c). Temperature profile for different values of We
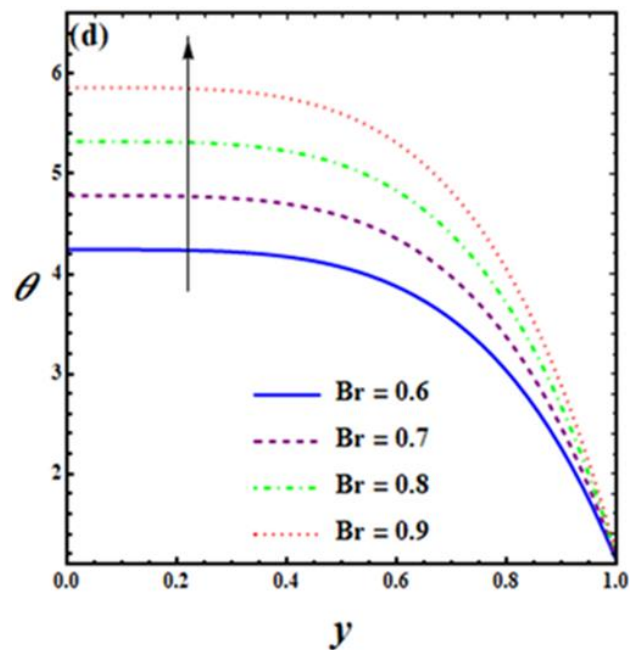
Fig. 3(d). Temperature profile for different values of Br
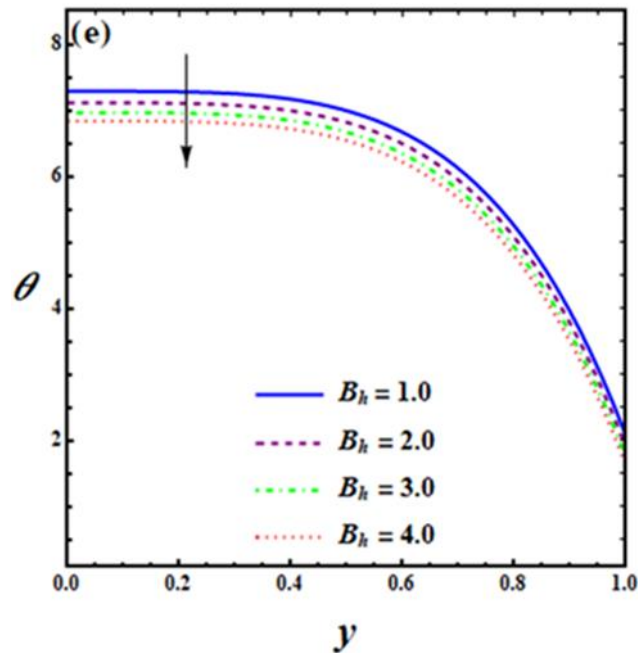
Fig. 3(e). Temperature profile for different values of B_h

3.3 Concentration Profile

This section explains the impact of different physical parameters on the concentration profile shown in Figure 4(a)-(g). The Figure 4(a) evaluate the variation of magnetic parameter on concentration which depicts the concentration of the particles increases by increasing values of Mn. The impact of the flow behavior index on the concentration profile shows in Figure 4(b). which shows the higher concentration by the higher value of n. Similarly, Figure 4(c) and 4(d) show the decreasing effect on the concentration profile by hiking values of the Weissenberg and Brickman parameters, respectively. The effect of the convective mass parameter on the concentration profile is explained in Figure 4(e), which shows a higher effect by increasing values of B_m. The variation of Schmidt and Soret parameters is explained on the concentration profile. Both show decreasing effect by increasing values of Sc and Sr i.e., Figure 4(f) and Figure 4(g) respectively.
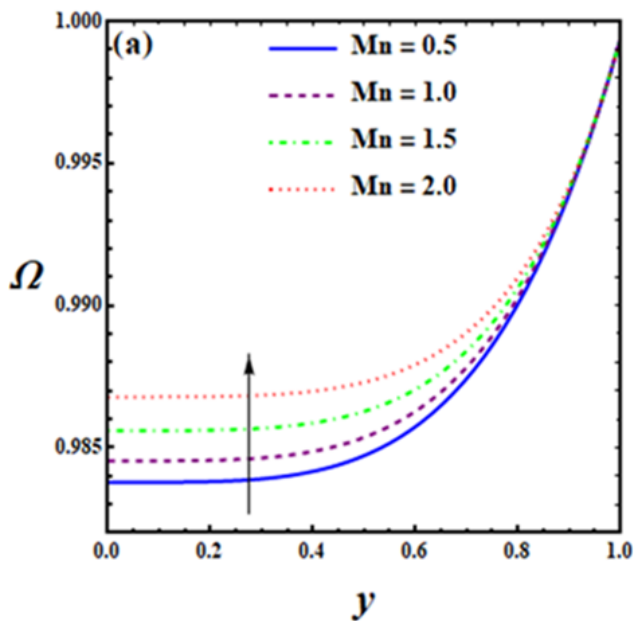
Fig. 4(a). Concentration profile for different values of Mn
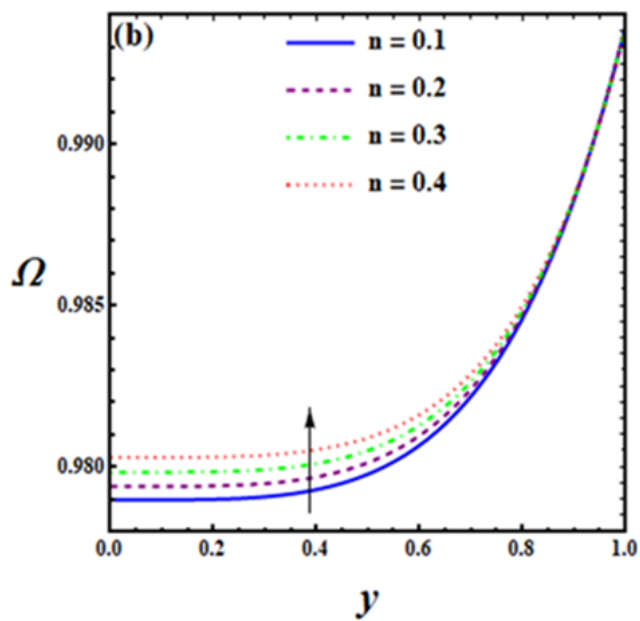
Fig. 4(b). Concentration profile for different values of n
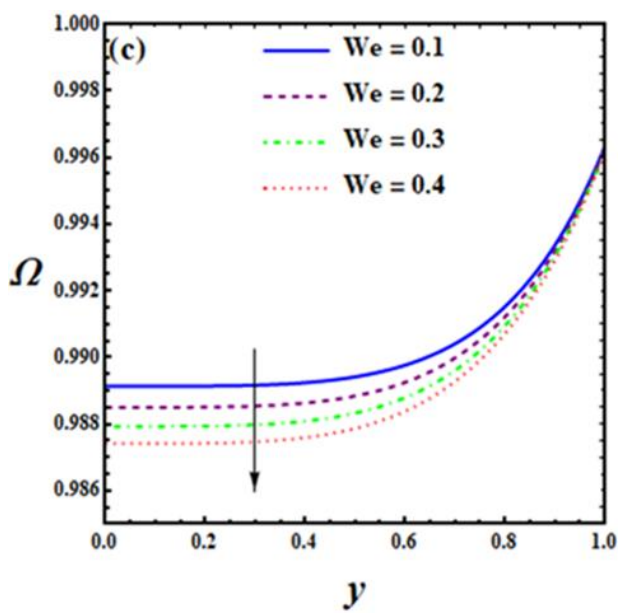
Fig. 4(c). Concentration profile for different values of We
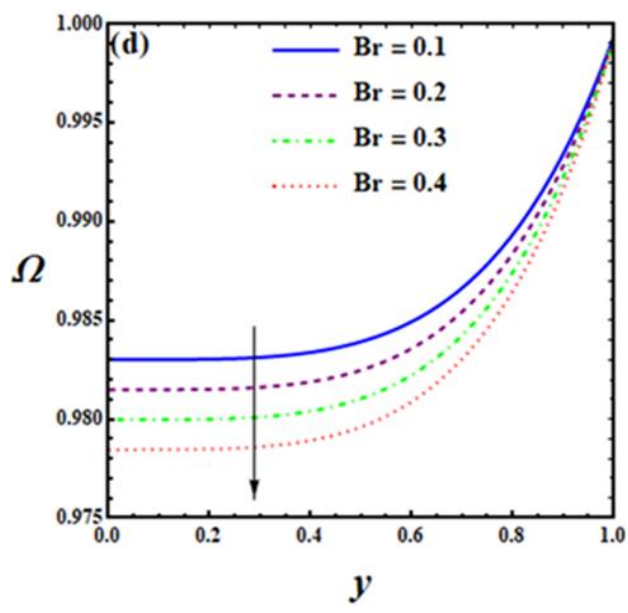
Fig. 4(d). Concentration profile for different values of Br
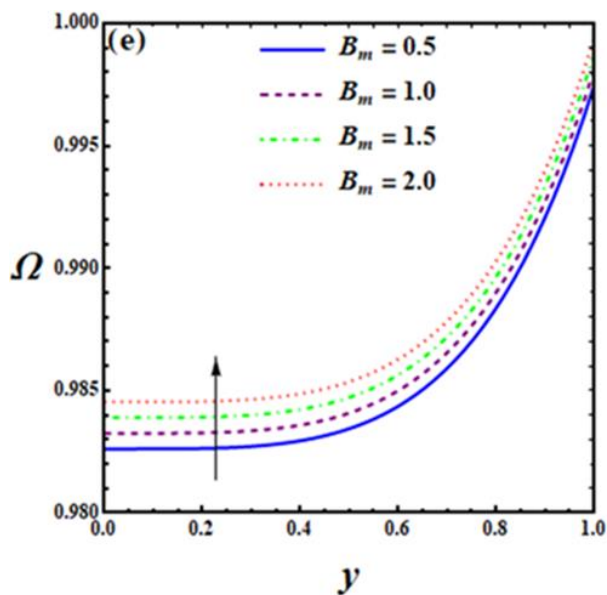
Fig. 4(e). Concentration profile for different values of B_m
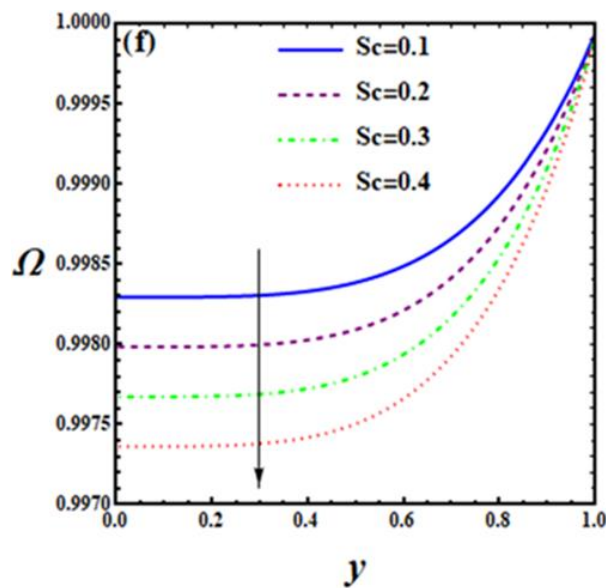
Fig. 4(f). Concentration profile for different values of Sc
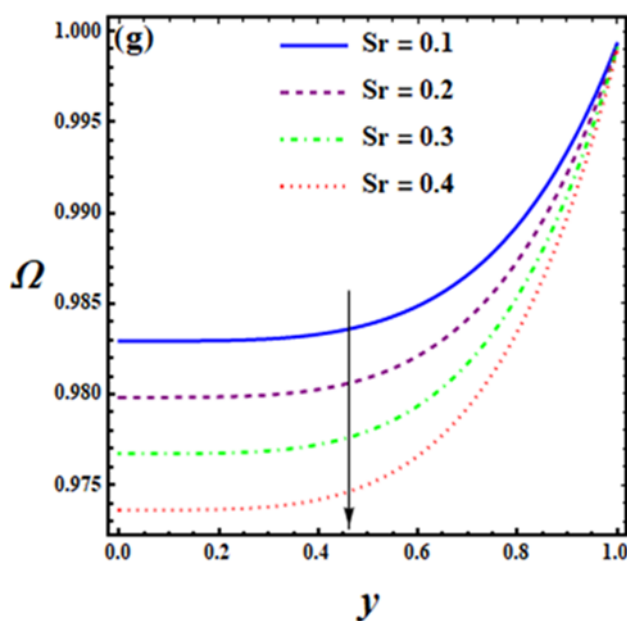
Fig. 4(g). Concentration profile for different values of Sr

3.4 Skin-Friction Coefficient, Nusselt Number and Sherwood Number

The numerical results of Skin friction coefficient C_f, Nusselt Number Nu and Sherwood Number are tabulated in Table 1, Table 2 and Table 3 respectively. Table 1 represents the calculated values of the Skin friction coefficient such as the magnetic parameter Mn, Flow index parameter n, Weissenberg parameter We and velocity slip parameter α. Varying the values of the Magnetic parameter shows a decreasing manner on C_f. The Skin friction coefficient's numerical outcomes increase by hiking the flow index parameter's value. A similar impact is demonstrated in the Weissenberg parameter, but a contrary variation was identified in the velocity slip parameter on skin friction.

Table 1
Skin-friction co-efficient for various values of (a) Mn (b) n (c) We (d) α

Mn	n	We	α	C_f
1.0	1.9	0.01	0.1	-7.76084
2.0				-17.2991
3.0				-20.6373
4.0				-24.4562
	1.0			-14.8952
	2.0			-14.8997
	3.0			-14.9042
	4.0			-14.9087
		0.01		-15.5753
		0.03		-15.1409
		0.05		-14.9663
		0.07		-14.9078
			0.1	-6.74026
			0.3	-7.84148
			0.5	-9.37296
		0.01	0.7	-11.6485
	1.9			
1.0				

Table 2
Nusselt number for various values of (a) Mn (b) n (c) We (d) Br (e) B_h

Mn	n	We	Br	B_h	Nu
1.0	1.9	0.01	0.5	1.0	-68.6629
2.0					-75.1317
3.0					-85.9174
4.0					-100.974
	1.0				-75.1305
	2.0				-75.1318
	3.0				-75.1332
	4.0				-75.1345
		0.01			-75.1317
		0.03			-75.1654
		0.05			-75.3402
		0.07			-76.1407
			0.6		-67.6185
			0.7		-60.1053
			0.8		-52.5922
			0.9		-45.0790
				1.0	-13.0303
				2.0	-18.2300
				3.0	-21.9330
			0.5	4.0	-24.8714
		0.01			
	1.9				
1.0					

A relevant physical parameter of the Nusselt number has been discussed through numerical outcomes in Table 2. The gradual growth of the magnetic and flow index parameters can reduce the Nusselt number's impact. Contrary behaviour was observed for the variation of the Brickman number on the Nusselt number. In continuing, the increasing manner of convective heat parameter reports the decreasing effect on Nu. Table 3 reports the interpretation of numerical data for the discrete physical constraints of Sherwood Number. In that, increasing order of Magnetic parameter and Flow index parameter shows the decreasing outcomes on Sherwood number. Transverse effect on Sherwood number observed by Weissenberg parameter and Brickman parameter. A growing order for Convective mass parameter predicts increasing growth on Sh. In continuing, by observing the numerical outcome of the Schmitt parameter and Soret parameter reports the growth of the Sherwood number.

Table 3
Sherwood number for various values of (a) Mn (b) n (c) We (d) Br (e) B_m (f) Sc (g) Sr

Mn	n	We	Br	B_m	Sc	Sr	Sh
1.0	1.9	0.01	0.5	1.0	0.1	0.1	-0.00591616
2.0							-0.00421997
3.0							-0.00296545
4.0							-0.00220848
	1.0						-0.00220784
	2.0						-0.00220782
	3.0						-0.00220756
	4.0						-0.00220637
		0.01					-0.00220848
		0.03					-0.00220975
		0.05					-0.00221746
		0.07					-0.00223162
			0.6				-0.00662452
			0.7				-0.01104120
			0.8				-0.01545630
			0.9				-0.01987140
				1.0			-0.00220872
				2.0			-0.00220869
				3.0			-0.00220864
				4.0			-0.00220856
					0.1		-0.02208050
					0.2		-0.04416050
					0.3		-0.06623810
					0.4		-0.08832370
						0.1	-0.02208050
1.0	1.9	0.01	0.5	0.1	0.1	0.2	-0.06623810
						0.3	-0.11040600
						0.4	-0.15456600

3.5 Trapping Phenomenon

This area explains the interior concept which explains the movement of the bolus that is produced in sinusoidal waveform on the walls of the channel, called the trapping phenomenon. Particularly, this section elaborates the impacts of various physical constraints such as Mn, n, We and α. The

bolus movement occurs with equal velocity as wave propagation of peristalsis. Figure 5(a). shows decreasing effect when compared with the width of the bolus which is produced by enhancing values of Mn. The flow behavior index's bolus movement also shows the same effect as Mn that drawn in Figure 5(b). Similarly, Figure 5(c). And Figure 5(d) elucidates the increasing and decreasing effect of bolus respectively.
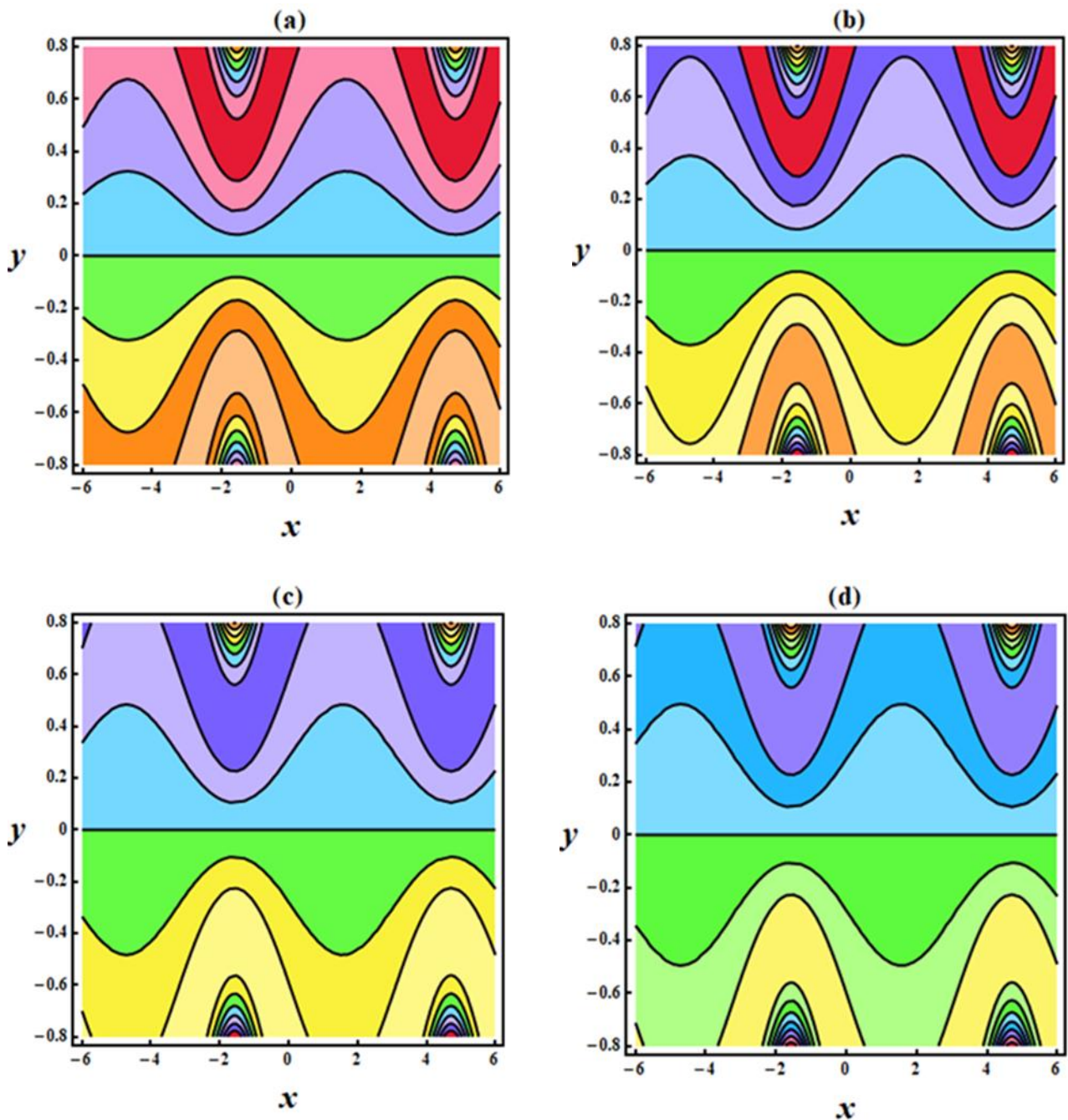
Fig. 5. Streamline graphs for different values of Mn
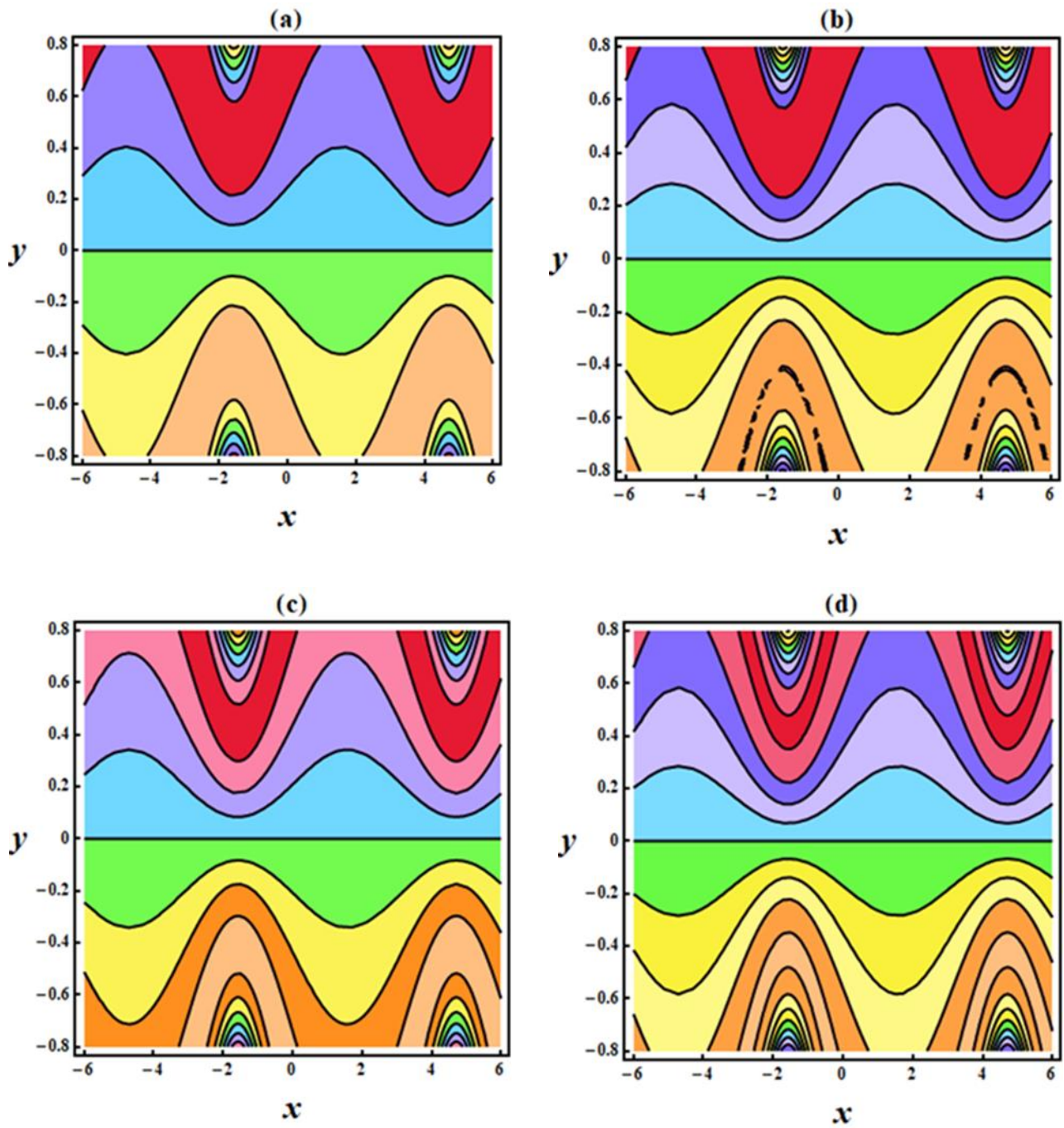
Fig. 6. Streamline graphs for different values of n
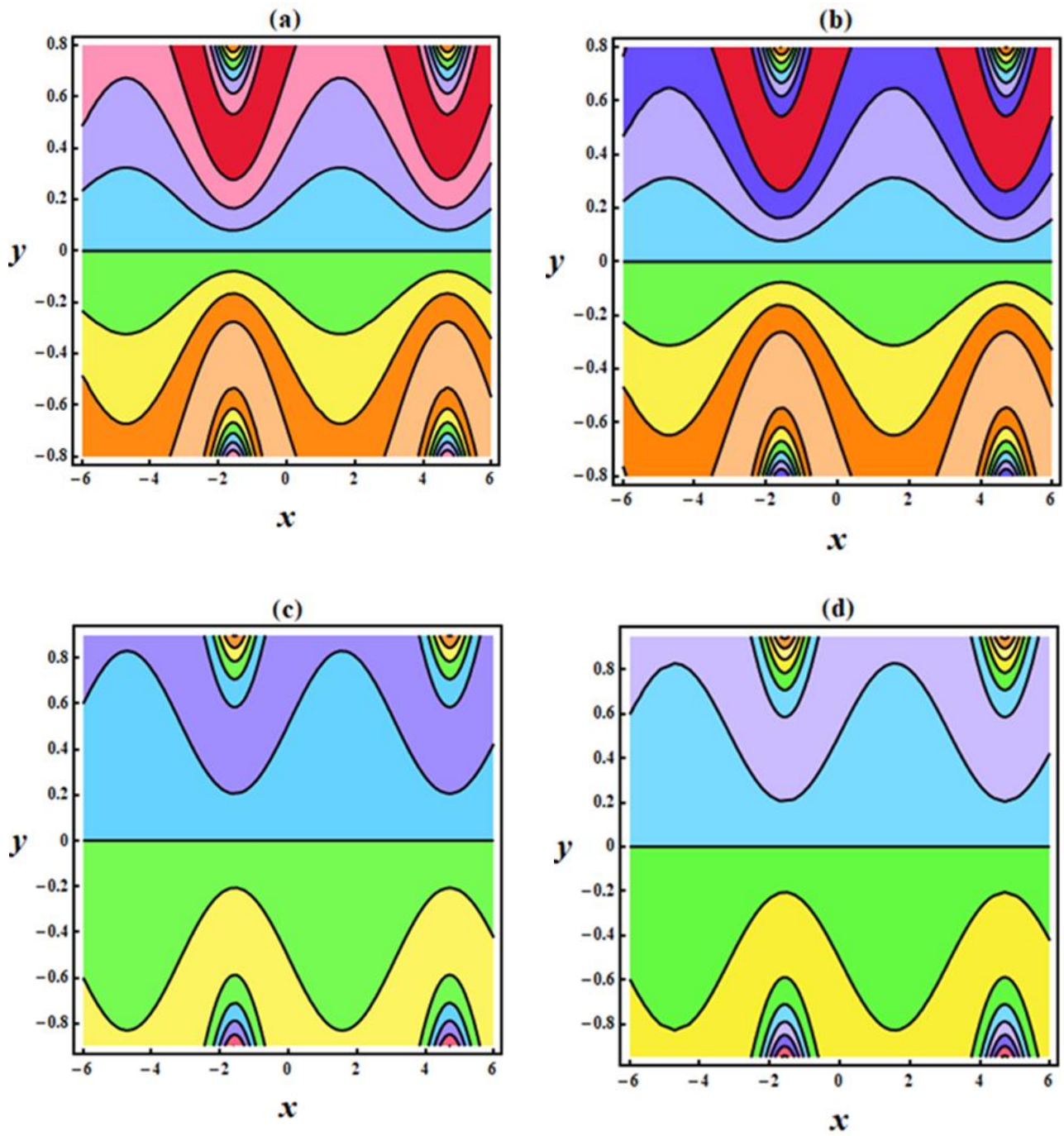
Fig. 7. Streamline graphs for different values of We
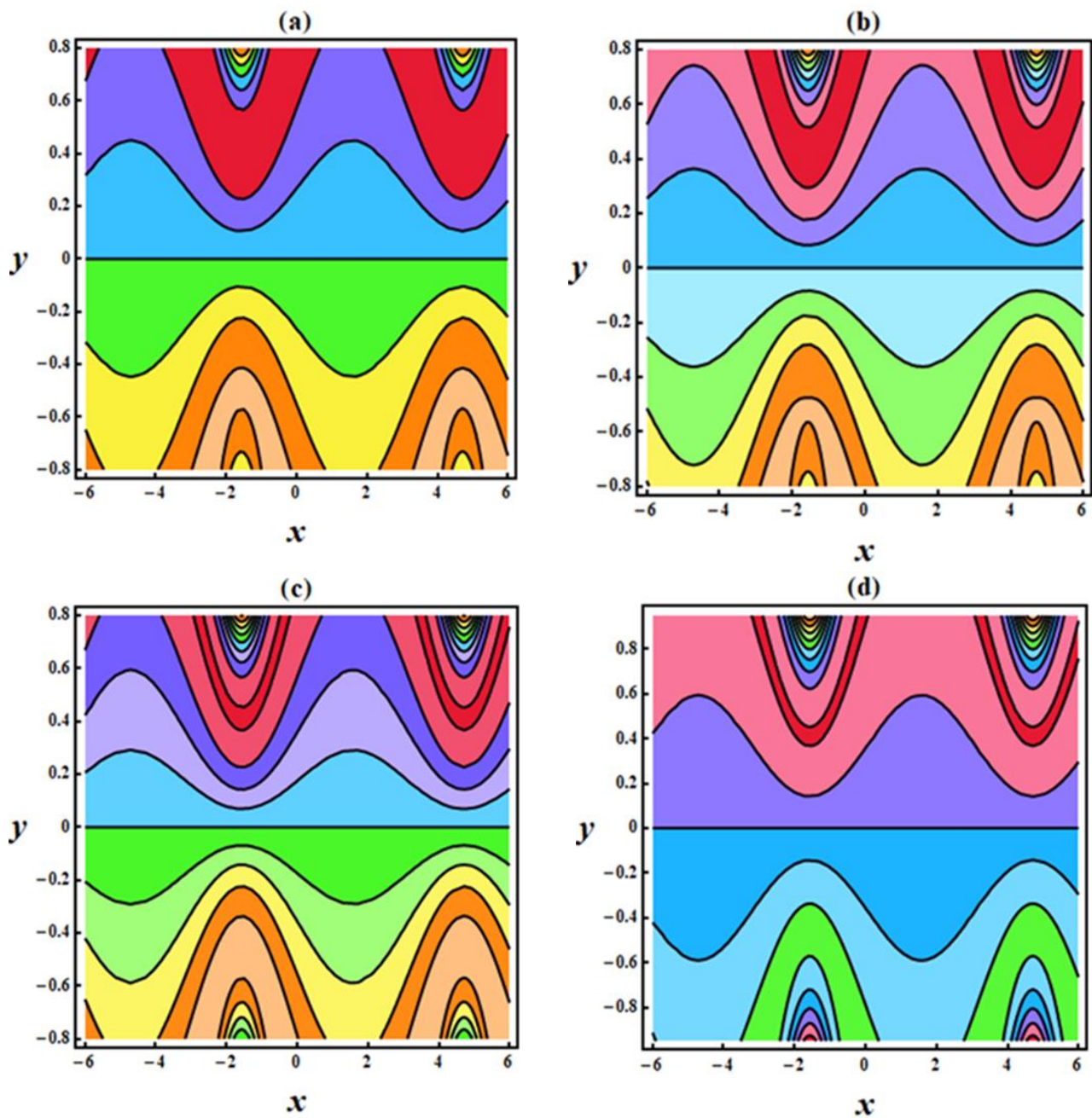
Fig. 8. Streamline graphs for different values of α

4. Validation

Figure 9 displays a graphical comparison between study [42], which forecasts fluid flow under the influence of the induced magnetic effect in the presence of partial slip boundary restrictions, and the current study. The present study is found to be consistent with study [42].
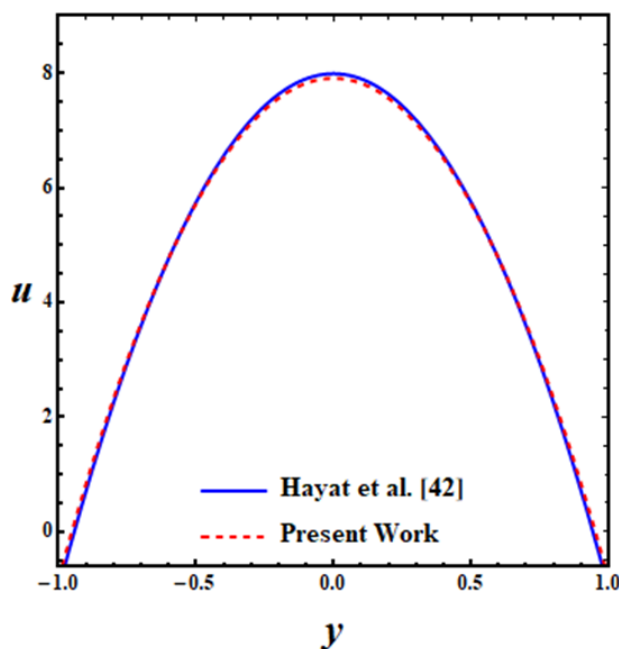
Fig. 9. Validation for Velocity

4. Conclusions

The peristaltic movement of non-Newtonian Carreau-Yasuda fluid is analysed through a planner micro-channel were formulated in the presence of an induced magnetic field (MHD) and appropriate partial boundary conditions. The impact of different physical parameters is investigated. The present article explores the significance of the Carreau-Yasuda fluid model in discrete areas such as industries, biomedical fields, and manufacturing areas. The significant outcomes of the current analysis are elaborated on below

i.   The greater value of the magnetic parameter shows a declining effect on velocity. Because the existence of Lorenz force shows resistance to the movement of the fluid. MHD plays a significant role during MRI, medical surgeries, cancer therapy, etc.
ii. The fluid flow on velocity predicts the declination when the velocity slip parameter is larger.
iii. The high value of the flow behaviour index explains the variation of fluid flow that shows the apparent fluid viscosity becomes high, due to which fluid faces more resistance.
iv. The higher flow index parameter controls both the velocity and temperature.
v.   The impact of convective heat and mass shows decreasing and increasing effects on temperature and concentration profiles, respectively, because the heat exchange is high in the concentration profile by the higher value of convective mass.
vi. The presence of a higher magnetic field shows the decreasing behaviour of the trapped bolus.

References

[1] Latham, Thomas Walker. "Fluid motions in a peristaltic pump." PhD diss., Massachusetts Institute of Technology, 1966.

[2] Burns, J. C., and T. Parkes. "Peristaltic motion." *Journal of Fluid Mechanics* 29, no. 4 (1967): 731-743. https://doi.org/10.1017/S0022112067001156

[3] Shapiro, Ascher H., Michel Yves Jaffrin, and Steven Louis Weinberg. "Peristaltic pumping with long wavelengths at low Reynolds number." *Journal of fluid mechanics* 37, no. 4 (1969): 799-825. https://doi.org/10.1017/S0022112069000899

[4] Raju, K. Kanaka, and Rathna Devanathan. "Peristaltic motion of a non-Newtonian fluid." *Rheologica Acta* 11, no. 2 (1972): 170-178. https://doi.org/10.1007/BF01993016

[5] Devi, Girija, and Rathna Devanathan. "Peristaltic motion of a micropolar fluid." In *Proc. Indian Acad. Sci*, vol. 81, pp. 149-163. 1975. https://doi.org/10.1007/BF03051177

[6] Srivastava, L. M., and V. P. Srivastava. "Peristaltic transport of blood: Casson model—II." *Journal of Biomechanics* 17, no. 11 (1984): 821-829. https://doi.org/10.1016/0021-9290(84)90140-4

[7] Vajravelu, Kuppalapalle, G. Radhakrishnamacharya, and V. Radhakrishnamurty. "Peristaltic flow and heat transfer in a vertical porous annulus, with long wave approximation." *International Journal of Non-Linear Mechanics* 42, no. 5 (2007): 754-759. https://doi.org/10.1016/j.ijnonlinmec.2007.02.014

[8] Srinivas, S., and M. Kothandapani. "The influence of heat and mass transfer on MHD peristaltic flow through a porous space with compliant walls." *Applied Mathematics and Computation* 213, no. 1 (2009): 197-208. https://doi.org/10.1016/j.amc.2009.02.054

[9] Waldrop, Lindsay, and Laura Miller. "Large-amplitude, short-wave peristalsis and its implications for transport." *Biomechanics and modeling in mechanobiology* 15 (2016): 629-642. https://doi.org/10.1007/s10237-015-0713-x

[10] Akbarzadeh, Pooria. "Peristaltic biofluids flow through vertical porous human vessels using third-grade non-Newtonian fluids model." *Biomechanics and modeling in mechanobiology* 17, no. 1 (2018): 71-86. https://doi.org/10.1007/s10237-017-0945-z

[11] Farooq, S., M. Ijaz Khan, T. Hayat, M. Waqas, and A. Alsaedi. "Theoretical investigation of peristalsis transport in flow of hyperbolic tangent fluid with slip effects and chemical reaction." *Journal of Molecular Liquids* 285 (2019): 314-322. https://doi.org/10.1016/j.molliq.2019.04.051

[12] Gijsen, F. J. H., E. Allanic, F. N. Van De Vosse, and J. D. Janssen. "The influence of the non-Newtonian properties of blood on the flow in large arteries: unsteady flow in a 90 curved tube." *Journal of biomechanics* 32, no. 7 (1999): 705-713. https://doi.org/10.1016/S0021-9290(99)00014-7

[13] Abbasi, Fahad Munir, Tasawar Hayat, Bashir Ahmad, and Guo-Qian Chen. "Peristaltic motion of a non-Newtonian nanofluid in an asymmetric channel." *Zeitschrift für Naturforschung A* 69, no. 8-9 (2014): 451-461. https://doi.org/10.5560/zna.2014-0041

[14] Abbasi, Fahad Munir, Tasawar Hayat, Bashir Ahmad, and Guo-Qian Chen. "Peristaltic motion of a non-Newtonian nanofluid in an asymmetric channel." *Zeitschrift für Naturforschung A* 69, no. 8-9 (2014): 451-461. https://doi.org/10.5560/zna.2014-0041

[15] Kayani, Sana Maryam, S. Hina, and M. Mustafa. "A new model and analysis for peristalsis of Carreau–Yasuda (CY) nanofluid subject to wall properties." *Arabian Journal for Science and Engineering* 45 (2020): 5179-5190. https://doi.org/10.1007/s13369-020-04359-z

[16] Javed, Muhammad Asif, Nasir Ali, Sabeen Arshad, and Shahbaz Shamshad. "Numerical approach for the calendering process using Carreau-Yasuda fluid model." *Journal of Plastic Film & Sheeting* 37, no. 3 (2021): 312-337. https://doi.org/10.1177/8756087920988748

[17] Ashraf, Hameed, Abdul Majeed Siddiqui, and M. A. Rana. "Flow analysis of Carreau fluid model induced by the ciliary cells, smooth muscle cells and pressure gradient at the ampullar region entrance." *Theory in Biosciences* 140, no. 3 (2021): 249-263. https://doi.org/10.1007/s12064-021-00352-8

[18] Gudekote, Manjunatha, Rajashekhar Choudhari, Hanumesh Vaidya, and Kerehalli Vinayaka Prasad. "Peristaltic flow of Herschel-Bulkley fluid in an elastic tube with slip at porous walls." *Journal of Advanced Research in Fluid Mechanics and Thermal Sciences* 52, no. 1 (2018): 63-75.

[19] Balachandra, H., Choudhari Rajashekhar, Hanumesh Vaidya, Fateh Mebarek Oudina, Gudekote Manjunatha, and Kerehalli Vinayaka Prasad. "Homogeneous and heterogeneous reactions on the peristalsis of bingham fluid with variable fluid properties through a porous channel." *Journal of Advanced Research in Fluid Mechanics and Thermal Sciences* 88, no. 3 (2021): 1-19. https://doi.org/10.37934/arfmts.88.3.119

[20] Khan, Mair, T. Salahuddin, and Rifaqat Ali. "An entropy flow analysis by means of new similarity approach." *International Communications in Heat and Mass Transfer* 129 (2021): 105642. https://doi.org/10.1016/j.icheatmasstransfer.2021.105642

[21] Hadimani, Balachandra, Rajashekhar Choudhari, Prathiksha Sanil, Hanumesh Vaidya, Manjunatha Gudekote, Kerehalli Vinayaka Prasad, and Jyoti Shetty. "The Influence of Variable Fluid Properties on Peristaltic Transport of Eyring Powell Fluid Flowing Through an Inclined Uniform Channel." *Journal of Advanced Research in Fluid Mechanics and Thermal Sciences* 102, no. 2 (2023): 166-185. https://doi.org/10.37934/arfmts.102.2.166185

[22] Waheed, S., S. Noreen, D. Tripathi, and D. C. Lu. "Electrothermal transport of third-order fluids regulated by peristaltic pumping." *Journal of Biological Physics* 46 (2020): 45-65. https://doi.org/10.1007/s10867-020-09540-x

[23] Alsaedi, A., Naheed Batool, H. Yasmin, and T. Hayat. "Convective heat transfer analysis on Prandtl fluid model with peristalsis." *Applied Bionics and Biomechanics* 10, no. 4 (2013): 197-208. https://doi.org/10.1155/2013/920276

[24] Abd-Alla, A. M., S. M. Abo-Dahab, A. Kilicman, and R. D. El-Semiry. "Effect of heat and mass transfer and rotation on peristaltic flow through a porous medium with compliant walls." *Multidiscipline Modeling in Materials and Structures* 10, no. 3 (2014): 399-415. https://doi.org/10.1108/MMMS-12-2013-0080

[25] Ahmad, Riaz, Asma Farooqi, Rashada Farooqi, Nawaf N. Hamadneh, Md Fayz-Al-Asad, Ilyas Khan, Muhammad Sajid, Ghulam Bary, and Muhammad Farooq Saleem Khan. "An analytical approach to study the blood flow over a nonlinear tapering stenosed artery in flow of Carreau fluid model." *Complexity* 2021 (2021): 1-11. https://doi.org/10.1155/2021/9921642

[26] Asghar, Z., and N. Ali. "Analysis of mixed convective heat and mass transfer on peristaltic flow of Fene-P fluid with chemical reaction." *Journal of Mechanics* 32, no. 1 (2016): 83-92. https://doi.org/10.1017/jmech.2015.56

[27] Shaheen, Aqila, and Muhammad Imran Asjad. "Peristaltic flow of a Sisko fluid over a convectively heated surface with viscous dissipation." *Journal of Physics and Chemistry of Solids* 122 (2018): 210-217. https://doi.org/10.1016/j.jpcs.2018.06.016

[28] Hayat, T., Farhat Bibi, S. Farooq, and A. A. Khan. "Nonlinear radiative peristaltic flow of Jeffrey nanofluid with activation energy and modified Darcy's law." *Journal of the Brazilian Society of Mechanical Sciences and Engineering* 41 (2019): 1-11. https://doi.org/10.1007/s40430-019-1771-2

[29] Latha, R., and B. Rushi Kumar. "Mass transfer effects on unsteady MHD blood flow through parallel plate channel with heat source and radiation." *JAEBS* 6, no. 5 (2016): 96-106.

[30] Prasad, Kerehalli Vinayaka, Hanumesh Vaidya, Gudekote Manjunatha, Kuppalapalle Vajravelu, Choudhari Rajashekhar, and V. Ramanjini. "Influence of Variable Transport Properties on Casson Nanofluid Flow over a Slender Riga Plate: Keller Box Scheme." *Journal of Advanced Research in Fluid Mechanics and Thermal Sciences* 64, no. 1 (2019): 19-42.

[31] Vaidya, Hanumesh, C. Rajashekhar, G. Manjunatha, K. V. Prasad, O. D. Makinde, and K. Vajravelu. "Heat and mass transfer analysis of MHD peristaltic flow through a complaint porous channel with variable thermal conductivity." *Physica Scripta* 95, no. 4 (2020): 045219. https://doi.org/10.1088/1402-4896/ab681a

[32] Salahuddin, T., Ahtsham Akram, Mair Khan, and Mohamed Altanji. "A curvilinear approach for solving the hybrid nanofluid model." *International Communications in Heat and Mass Transfer* 137 (2022): 106179. https://doi.org/10.1016/j.icheatmasstransfer.2022.106179

[33] Salahuddin, T., Abdul Mosan Bashir, and Mair Khan. "Numerical study on thermal performance of TiO2, Fe3O4 and NiCr/engine oil in an inclined wavy pip." *Journal of the Indian Chemical Society* 99, no. 11 (2022): 100719. https://doi.org/10.1016/j.jics.2022.100719

[34] Navier, C. L. M. H. "Sur les lois du mouvement des fluids, Mem." *Acad. Roy. Sci. Inst. Fr* 6 (1827): 389-440.

[35] Vaidya, Hanumesh, and Kerehalli Vinayaka Prasad. "Significances of homogeneous-heterogeneous reactions on casson fluid over a slippery stretchable rotating disk with variable thickness." *CFD Letters* 11, no. 4 (2019): 41-63.

[36] Baliga, Divya, Manjunatha Gudekote, Rajashekhar Choudhari, Hanumesh Vaidya, and Kerehalli Vinayaka Prasad. "Influence of velocity and thermal slip on the peristaltic transport of a herschel-bulkley fluid through an inclined porous tube." *Journal of Advanced Research in Fluid Mechanics and Thermal Sciences* 56, no. 2 (2019): 195-210.

[37] Hussin, Norasikin, Siti Shareeda Mohd Nasir, Nor Azirah Mohd Fohimi, Rohidatun Mahmod, Yusli Yaakob, and Dzullijah Ibrahim. "Analysis of Thermal Comfort and Energy Consumption for Educational Building." *Journal of Advanced Research in Experimental Fluid Mechanics and Heat Transfer* 10, no. 1 (2022): 1-9.

[38] Khan, Ambreen Afsar, Rahmat Ellahi, and Muhammad Usman. "The effects of variable viscosity on the peristaltic flow of non-Newtonian fluid through a porous medium in an inclined channel with slip boundary conditions." *Journal of Porous media* 16, no. 1 (2013). https://doi.org/10.1615/JPorMedia.v16.i1.60

[39] Afzal, Khadeeja, and Asim Aziz. "Transport and heat transfer of time dependent MHD slip flow of nanofluids in solar collectors with variable thermal conductivity and thermal radiation." *Results in physics* 6 (2016): 746-753. https://doi.org/10.1016/j.rinp.2016.09.017

[40]   Salahuddin, T., Muhammad Habib Ullah Khan, Mair Khan, Basem Al Alwan, and Abdelfattah Amari. "An analysis on the flow behavior of MHD nanofluid with heat generation." *Fuel* 311 (2022): 122548. https://doi.org/10.1016/j.fuel.2021.122548

[41]   Salahuddin, T., Abdul Mosan Bashir, Mair Khan, Basem Al Alwan, and Mohammad Almesfer. "Hybrid nanofluid analysis for a class of alumina particles." *Chinese Journal of Physics* 77 (2022): 2550-2560. https://doi.org/10.1016/j.cjph.2021.11.012

[42]   Hayat, T., Humaira Yasmin, and A. Alsaedi. "Peristaltic motion of Carreau fluid in a channel with convective boundary conditions." *Applied Bionics and Biomechanics* 11, no. 3 (2014): 157-168. https://doi.org/10.1155/2014/571689